NATURAL CONVECTION HEAT TRANSFER IN CLOSED VESSELS WITH INTERNAL HEAT SOURCES -- ANALYTICAL AND EXPERIMENTAL STUDY

Frederick G. Hammitt

Associate Professor
Departments of Mechanical and Nuclear Engineering
The University of Michigan

IP-314

August, 1958

ACKNOWLEDGEMENTS

The writer wishes to thank Elayne M. Brower, Research Assistant, for her very great help in operating the computer program, reducing experimental data, and running the experiments.

TABLE OF CONTENTS

INTRODUCTION

The phenomenon of natural convection heat transfer and fluid flow in closed vessels with heat sources internal to the fluid has assumed importance in connection with homogeneous nuclear reactors. It is also prominent in various chemical processes. Natural convection, in the absence of internal heat sources perhaps under the impetus of an intensified body force, is important also in various applications.

This paper presents the results of an experimental and analytical study on vertical, cylindrical closed cells, containing fluid in which heat is generated internally. The heat is removed through the container walls to maintain steady state. As a special case the analysis is applicable to the condition of no internal heat generation; rather replenishment through open access at one end to an infinite reservoir. It gives a basis for engineering estimates of temperature differentials, velocities, and heat fluxes.

The analysis has been conducted in terms of various non-dimensional parameters which are defined in the nomenclature. Chief among these are the non-dimensional heat source, q_V, which is considered to be radially uniform but may vary axially; the non-dimensional temperature differential, t, between vessel centerline and wall; and the non-dimensional wall temperature differential between the wall at any point and the wall at the bottom of the vessel. The variation of wall temperature is arbitrary in the axial direction.

The heat source term, q_V, is directly proportional to the volumetric heat source rate and to the vessel radius to the sixth power; inversely to the vessel length. It also involves various of the physical properties. The phenomenon within a closed cell is completely described by the non-dimensional heat source alone if the wall temperature distribution is given. This is because of the recirculating nature of the flow which does not allow an independent specification (once heat source is specified) of the fluid temperature at any point. However, a given q_V value may apply either to a vessel of large diameter with moderate heat source or to a vessel of small diameter and large heat source (as some power reactor designs).

The analysis covers q_V from approximately 10^2 to 10^9, losing its physical applicability below about 10^2. There is, however, no corresponding upper limit imposed. The experimental results include the q_V range between 10^7 and 10^{10}. Various wall temperature and heat source distributions have been covered. The degree of agreement between analysis and theory and the applicability of the results is discussed in the paper and under Conclusions.

ANALYSIS

The method of analysis follows the approach employed by Lighthill.[1] It is generalized to include an internal heat source. In addition, arbitrary axial variation of the internal heat source and the wall temperature is allowed. Finally, the analysis is modified to that of a vessel closed at both ends so that the condition of re-circulation of the fluid with energy conservation is required at each end.

Following reference 1 the present analysis requires the conservation of energy, momentum, and mass for any radial cross-section, though not on a point to point basis. Radial temperature and velocity profiles are assumed which meet the physically required boundary conditions and their first derivatives at the wall, the centerline, and the interface between upward and downward flowing streams. Further assumptions implicit in the analysis are that the Prandtl Number of the fluid be of the order unity, that the partial derivatives of all quantities normal to the wall be large compared with those in the axial direction, and that the flow be laminar. The Prandtl Number assumption is used to neglect inertial terms when compared with viscous terms* and also to assign an equal radial extent to temperature and velocity profile features. The assump tion regarding the partial derivatives (boundary layer assumption) is applicable to any q_v.

---

* This approximation has been investigated in detail.[6] It appears applicable for fluids with Prandtl Number near unity and above but not for liquid metals.

With somewhat more restrictive conditions Lighthill[1] obtained an exact solution. This did not appear possible in the present case. Hence a numerical procedure was adopted and programmed for an IBM-650 digital computer. The detailed steps of the analysis and the preliminary machine results are given in a previous paper by the present author.[2]

The assumed velocity and temperature profiles are shown in Figure 1, and these are generally in agreement with the experimental observations. The hypothesized flow is characterized by a layer consisting mainly of descending flow adjacent to the wall wherein velocity varies rapidly as a function of radius, and an ascending core wherein velocity is not a function of radius. The temperature profile shows a severe gradient close to the wall covering a radial extent equal to that of the velocity boundary layer, and a constant temperature across the core. It develops both analytically and experimentally that the thickness of the boundary layer, at a given relative axial position increases with decreasing q_v. A final lower limit to the applicability of this analysis then develops when the boundary layer fills the entire vessel. Depending upon the wall temperature distribution this occurs for a q_v between 10^2 and 10^3.[5]

Also, in general the boundary layer grows from small thickness near the top of the vessel to a maximum near the bottom. Thus the upper portion is in a sense analogous to the entry section of a pipe wherein the boundary layer is not yet fully developed. For q_v less than the above limit, the flow in the central and lower portion of the vessel would be somewhat analogous to the fully-developed portion of a pipe flow and can

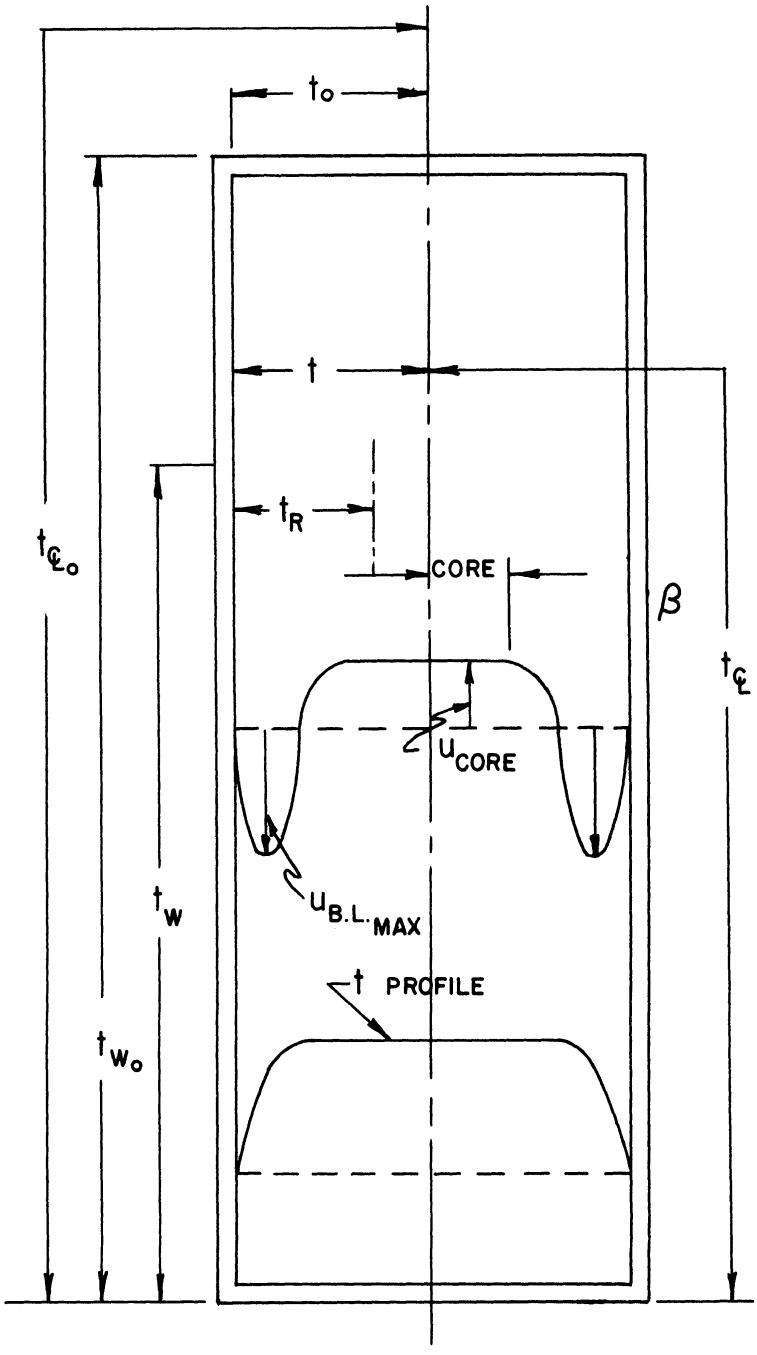

Figure 1. Test Section Nomenclature Schematic.

in fact be analysed on the basis of no parameter variation in the axial direction for this portion. The present paper, however, considers only q_v values above this lower limit.

The question of the physical occurrence of flows of the type described by this theory is made somewhat doubtful by the possible non-existence of streamline flow over the applicable q_v range. For large q_v the assumed constant temperature and velocity in the ascending core is closely realized, since the boundary layer is confined to the region immediately adjacent to the wall. However, for the large q_v range, in vessels of length greater than radius, turbulence is inevitably encountered. For small q_v where laminar flow might be expected the applicability of the assumed profiles is less certain. Nevertheless, the correlation achieved between theoretical and experimental results shows that the analysis gives a useful guide to the degree and direction of variations to be expected as the independent parameters are changed.

EXPERIMENTAL APPARATUS

The experimental data upon which this paper is based have been derived from several pieces of apparatus which are similar in basic fundamentals. In all cases heat is generated by ohmic resistance in an aqueous solution contained within a vertical, cylindrical, glass vessel; and in all cases heat is removed through the containing wall. In two of the cases the heat removal is by forced convection water flow, in the other by natural convection air. In all cases, temperature is measured at a point within the fluid by a glass-encased thermocouple probe leaving a very small bead exposed to the fluid. Velocities are estimated by timing the motion of dye injected at a known location.

The major portion of the data results from the water-cooled facility illustrated in Figure 2. A cross-section drawing is shown in Figure 3. Basically the glass test section is held between carbon-steel electrodes at either end. The main structural support is a large glass cylinder which also contains the cooling water. The test section is not a suitable support because minimum wall thickness is required to allow a maximum heat flux without boiling.

A plexiglas baffle-cylinder surrounds the test section leaving a 1/4 inch annulus for forced-convection water cooling. The arrangement allows the substitution of test sections of different lengths. Lengths varying between 22-1/4 inches and 6-1/4 inches were used. In all cases the test section inside diameter was 3-7/8 inches.

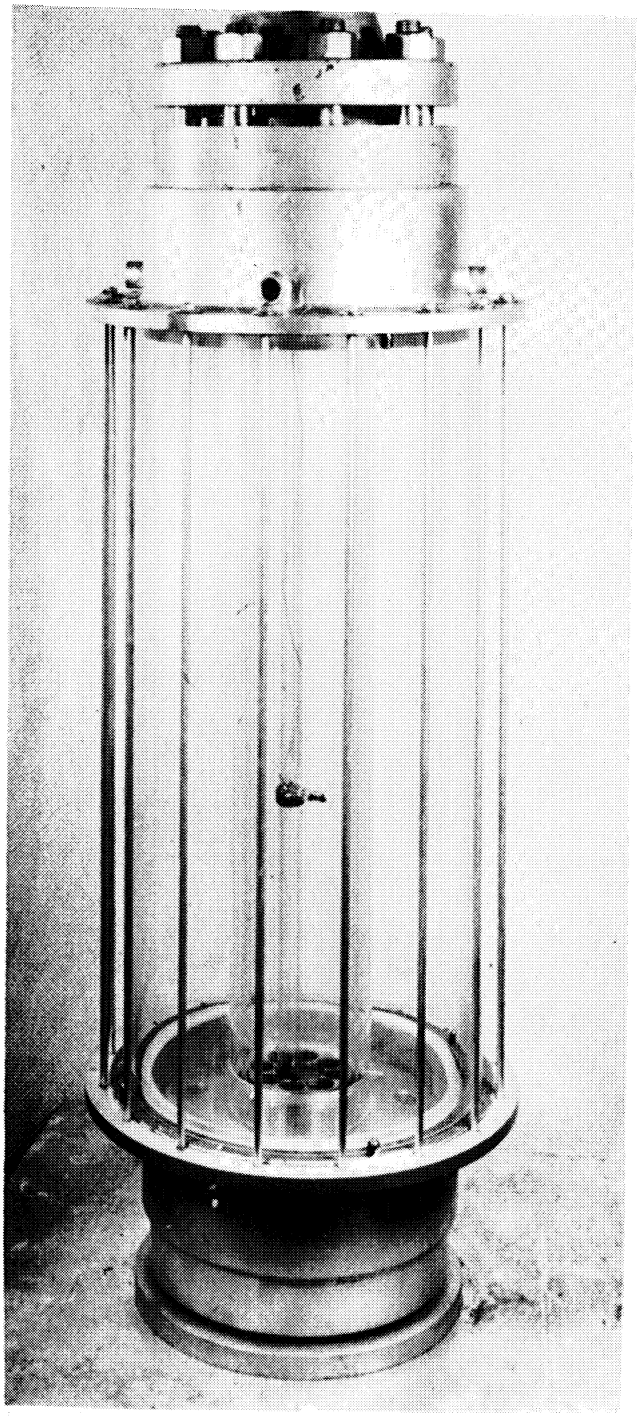

Figure 2. Photograph of Water-Cooled Facility.

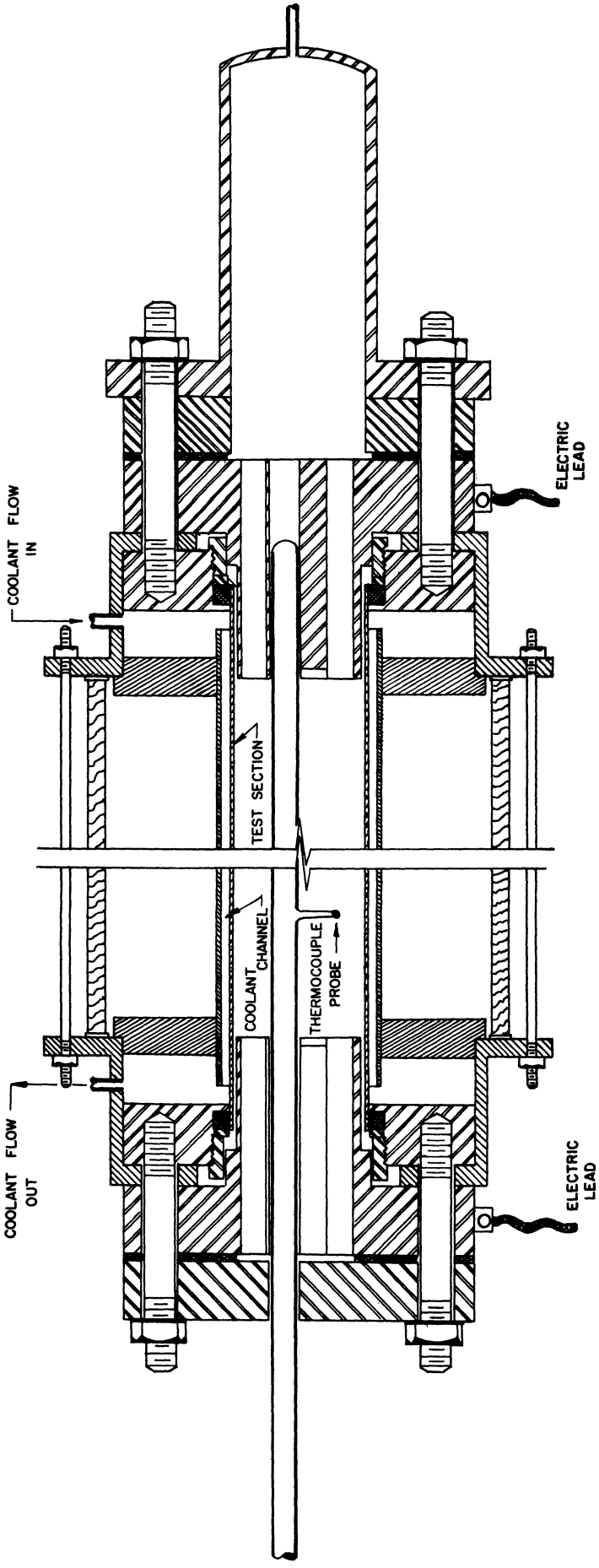

Figure 3. Layout Drawing of Water Facility.

An eccentric 3/4 diameter vertical glass tube guided by bushings in the electrodes was used as the support for the thermocouple and dye-injection head. This component can be viewed in Figures 2 and 3. The thermocouple and dye-injection heads are in effect projections perpendicular to the vertical tube of such a length that they touch the wall on the near side, as governed by the eccentricity of the vertical tube, and reach a certain maximum displacement from the wall on the opposite side. The vertical tube can be moved in the axial direction. Hence, if axially symmetrical flow is assumed, it is possible to obtain a complete temperature and qualitative velocity survey of the test section.

Magnitude and direction of coolant flow, heat input rate, and test section dimensions were the independent variables subject to control. Heat inputs ranging between approximately 300 watts and 2500 watts were utilized in the various tests. A maximum of about 4000 watts could be attained without boiling. The power source was 220 volt, 60 cycle, single phase alternating current controlled through a variable ratio transformer. Coolant rates ranged between approximately 0.15 GPM and 10 GPM. At a given power input rate, the coolant rate and direction of flow influenced the wall temperature distribution and thus provided different test points. A heat balance on the coolant was taken and found to match the electrical input within the experimental accuracy.

A second source of test results was a smaller scale apparatus cooled by natural convection with atmospheric air. In this case, the only independent variables were power input and test section dimensions.

The test section diameter was 2-5/8 inches and the length varied between 20 inches and 7-3/4 inches for the various tests. Power inputs ranged between approximately 10 and 100 watts. Local temperatures were measured by a glass thermocouple probe consisting of a 3/16 inch diameter glass tube sealed around the wires in such a manner that a small bead protruded. Dye injection was utilized to estimate magnitudes and directions of velocity. Wall heat flux at local points was estimated by measuring the outer wall temperature by attached thermocouples.

The air-cooled and water-cooled facilities are described in detail in reference 3.

A third source of data was provided by several tests in a water-cooled facility similar in principle to that described above which was utilized in tests at Oak Ridge and is described in reference 4. These provide data in a q_v range somewhat larger than that attained in the tests described in this paper, and hence are a useful addition to the data. In this case the test section diameter was 6 inches and the length was 24 inches.

EXPERIMENTAL AND ANALYTICAL RESULTS

General Objectives

Experimental measurements of temperatures, estimations of velocities, and observations on the type of flow, i.e. laminar or turbulent, have been made under a variety of test conditions. These include test section diameters ranging from 2-5/8 inches to 6 inches, lengths from 6 to 24 inches, and length to diameter ratios from about 2 to 8. Heat inputs ranged from about 10 to 2500 watts. The ratio between the temperature differential from wall to centerline across the top to the differential between centerline at top and wall at bottom varied between about 2 and 40.

A laminar flow analysis, providing values for local temperature, velocity, and wall heat flux under conditions of arbitrary axial wall temperature and heat source distribution has been evolved. The endeavor of this investigation has been to compare the analytical and experimental results in all possible details so as to prepare a basis for the engineering prediction of the significant quantities under conditions not covered by the experiments.

Anticipated Discrepancies between Experiments and Analysis

The analysis has been based on an axi-symmetric, laminar flow regime wherein the fluid physical properties may be considered constant. None of these requirements of course are met in detail so that some discrepancy between analysis and experiment is to be expected. The most

important factor in this respect is believed to be the presence of a slow eddying motion rather than streamline flow in almost all experiments, most particularly in those with large Rayliegh Number based on radius. This "turbulence" was observed visually with dye. It was also noted through its effect on the temperature readings which oscillated continually with a period of the order of perhaps 30 seconds for the more turbulent runs. The time interval may well be associated more with the period of the instrumentation (a precision potentiometer) than with the flow.

In a given test section, as power is increased, turbulence first appears near the top in the central portion. As the heat input is further increased it encompasses an increasing portion of the vessel. The bottom, where velocities are at a minimum, is affected last.

It would be intuitively expected that the radius Rayleigh Number would be closely associated with the appearance of turbulence in a test section of this type. This is indeed the case with large scale turbulence appearing above a radius Rayleigh Number, Ra_a, of about 4.0×10^7. It appears questionable that Ra_a can be considered the only significant factor. Since there are some inconsistencies in the data from this viewpoint, further research is desirable.

Most of the tests involved a large degree of turbulence. Further, it cannot be assured that true streamline flow existed in all portions of the vessel for any of the tests. Hence it is to be expected that the temperature differential necessary to motivate a given rate of heat flow will be less than that calculated. This was actually the case.

Of less importance than the laminar-turbulent issue is that of the assumption of constant fluid physical properties throughout. The most temperature-dependent property is the viscosity. This shows a maximum 2:1 change between the highest and lowest temperature portions of the test section. Values corresponding to an approximately weighted mean temperature were used. It is difficult with the present limited knowledge of the phenomenon to estimate the discrepancies which may have been caused on this account.

A final obvious cause of discrepancy between theory and experiment is the assumption of axial symmetry. The flow pattern observed in these tests was that of a single circulating cell with a rising fluid core in the center and a descending layer along the wall. No tangential velocities were observed at any time.

By the nature of the eccentric thermocouple probe it was not possible to obtain temperature measurements at a given radius at more than one angular position. However, a sharp temperature gradient adjacent to the wall with a flat profile across the remainder of the vessel was obtained in all cases and at all axial positions. Typical experimental points are shown in Figure 4. It does not seem possible that such data would be obtained unless axial symmetry was substantially in existence. In several cases tests were conducted with and without the thermocouple probe in the vessel. No difference in the fluid behavior or in the overall temperature differential between end plates was found. Local fluid temperatures could not of course be measured in the absence of the probe.

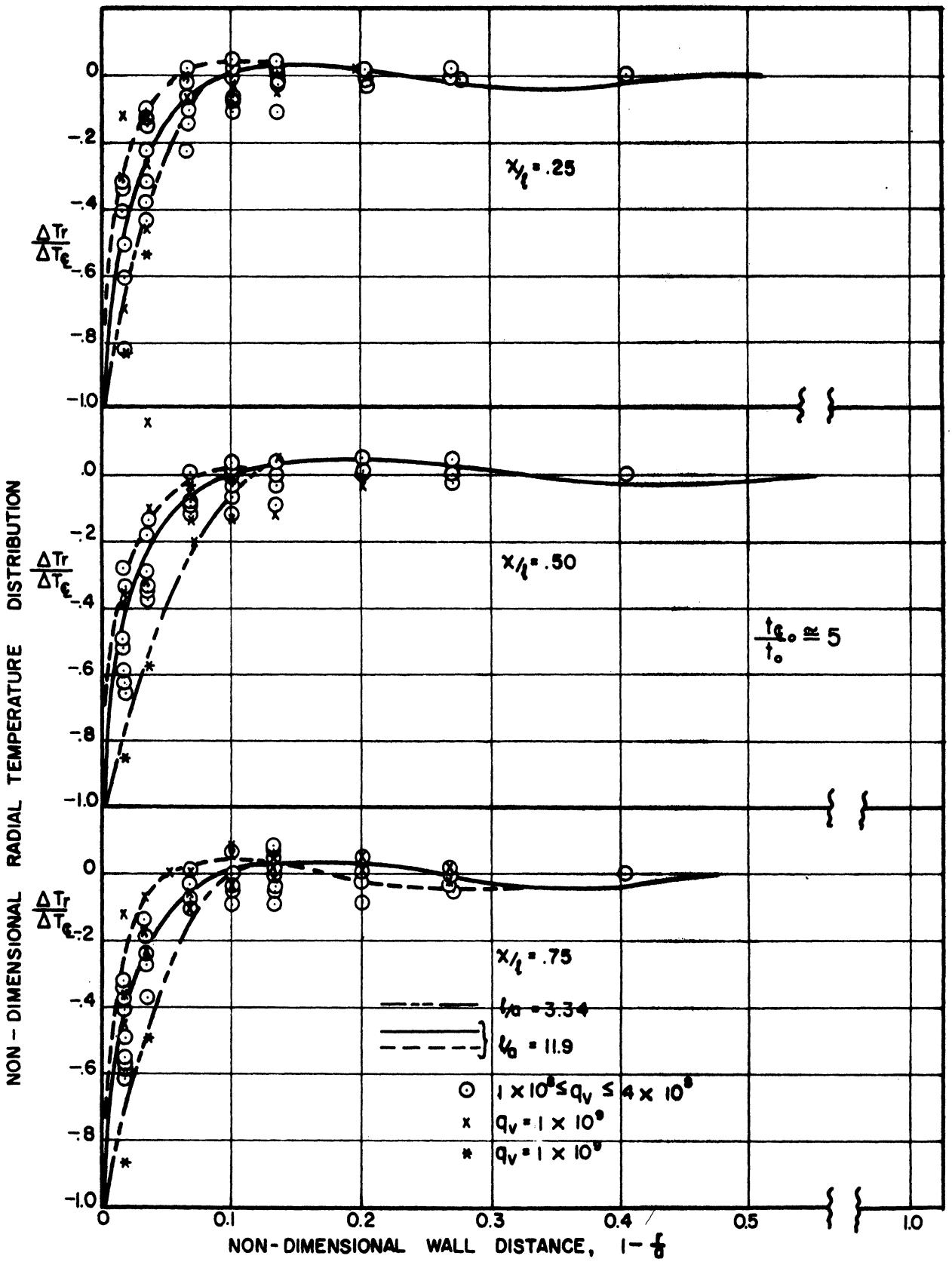

Figure 4. Radial Temperature Distribution - Experimental Data.

The eccentric probe could also influence the flow by adding shear area and blocking flow area. The blockage of flow area is less than 5% and hence probably not important. The increase in shear area is of the order of 18%. However, the core velocities are small compared with those in the descending fluid adjacent to the wall so that the shear forces on the probe are probably not of great importance.

Comparisons between Analytical and Experimental Data

Overall Comparison

A comparison between overall heat transfer parameters as measured experimentally and as predicted by the analysis is probably most important. Figure 7 summarizes such a comparison, and also shows analytical predictions over a q_v range much greater than that observed experimentally. A variety of wall temperature and heat source distributions are shown.

The results are presented in terms of the non-dimensional heat source, q_v, and the non-dimensional temperature differential between the fluid at the centerline at the top and the wall at the bottom, $t\not{\epsilon}_o$. These quantities are algebraically related to Nusselt's Number based on tube radius in the following way:

$$Nu_a = q_v/2t\not{\epsilon}_o$$

Hence the data of Figure 7 could be cross-plotted to show the relation between q_v or $t\not{\epsilon}_o$ and Nu_a.

The parameter attached to the curves describes both the wall temperature and heat source distributions. The following cases have been

covered by the calculations and are shown on the curves:

1) Constant wall temperature

   a) Uniform heat source.

   b) Linear axial variation of heat source - maximum at top, zero at bottom - designated ▽ on curves.

   c) Linear axial variation of heat source - maximum at bottom, zero at top - designated △ on curves.

   d) Sine axial distribution of heat source - maximum in center, zero at ends.

   e) Heat source concentrated in differentially thin radial disc across bottom - designated ⌊ on curves. This is equivalent to the assumption of the bottom end open to an infinite reservoir and hence should check the results of reference 1. A comparison will show that it does.

2) Variable Wall Temperature

   Linear Variation. The wall temperature is assumed to decrease linearly from top to bottom. The magnitude of the decrease is expressed in terms of the ratio between temperature differential across the top of the vessel plus that down the wall to the differential across the top only, $\frac{t_{\ell o}}{t_o}$. The curves are so labeled. For constant wall temperature this ratio becomes unity. To this writing, the calculations have been limited to values of the ratio of unity or greater.

A temperature distribution closely matching that measured in the various tests was also computed to estimate the degree of variation from the linear case. It was found that the variation was negligible, hence it appears that the exact shape of the temperature gradient is not of great importance.

As noted, the range of q_v examined analytically is from approximately 10^2 to 10^9.

The curves of q_v vs t_{ℓ_o} are virtually straight lines over the entire range if plotted on logarithmic co-ordinates. Thus curve fitting relations of the type $q_v = k\, t^n_{\ell_o}$ can be given for the various wall temperature and heat source distributions and are accurate over a reasonable range of q_v. The value of the exponent, n, for all the computed curves is quite close to 1.25 a value which is typical of most natural convection analyses. The exponent for the experimental curves is somewhat greater, ranging between about 1.3 and 1.5. The increased steepness of the curves means a reduced temperature differential to remove a given quantity of heat for higher q_v. It is felt that this is the result of increased turbulence.

The computed curves are terminated as a lower limit at a q_v ranging between 10^2 and 10^3 depending on the temperature distribution. It is at this point that the type of analysis loses significance since the boundary layer fills the entire vessel at some point along the length. A further extension would entail negative core thicknesses. This situation is examined in reference 5. The details of the calculations for higher q_v and the detailed listing of the experimental data are found in reference 3.

The experimental data cover the range between q_v of 10^7 and 10^{10}. Figure 5 shows the experimental points for the 47 runs from the three sets of apparatus previously described. At various q_v, $t_{\not{c}_o}$ is plotted against the ratio $t_{\not{c}_o}/t_o$. The three points for the values of this ratio of about 32, 42, and 49 result from the experiments described in reference 4. These were actually taken at a q_v of about 10^{10}. They have been prorated to the lower q_v values using the theoretical (laminar-flow) curves. Hence the experimental data at high values of $t_{\not{c}_o}/t_o$ cannot be considered too seriously and were not included in Figure 7. The curves of Figure 5 are cross-plotted to form the experimental curves of Figure 6. These are incorporated in Figure 7 where the calculated data are also shown.

A comparison of the experimental and theoretical curves in Figure 7 shows an increasing discrepancy in the direction of a decreased temperature differential for a given heat source as the heat source rate is increased. The factor is of the order of 1.5 for the lower and 2.5 for the larger q_v. It would be expected to become approximately unity for still lower q_v, although no further data are available at the present writing.

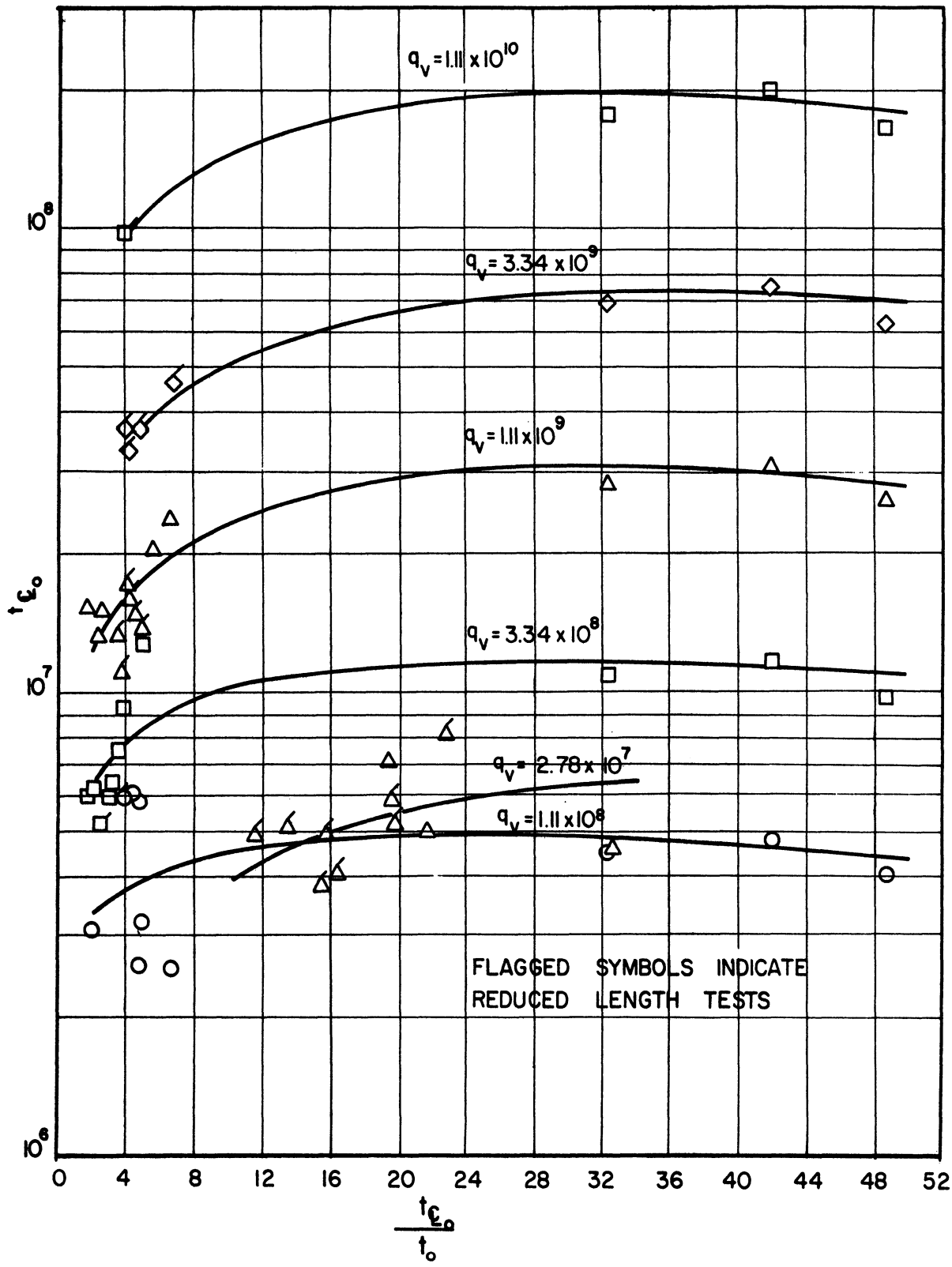

Figure 5. Non-Dimensional Overall Temperature Difference vs. Overall/Radial Temperature Ratio, Experimental Data.

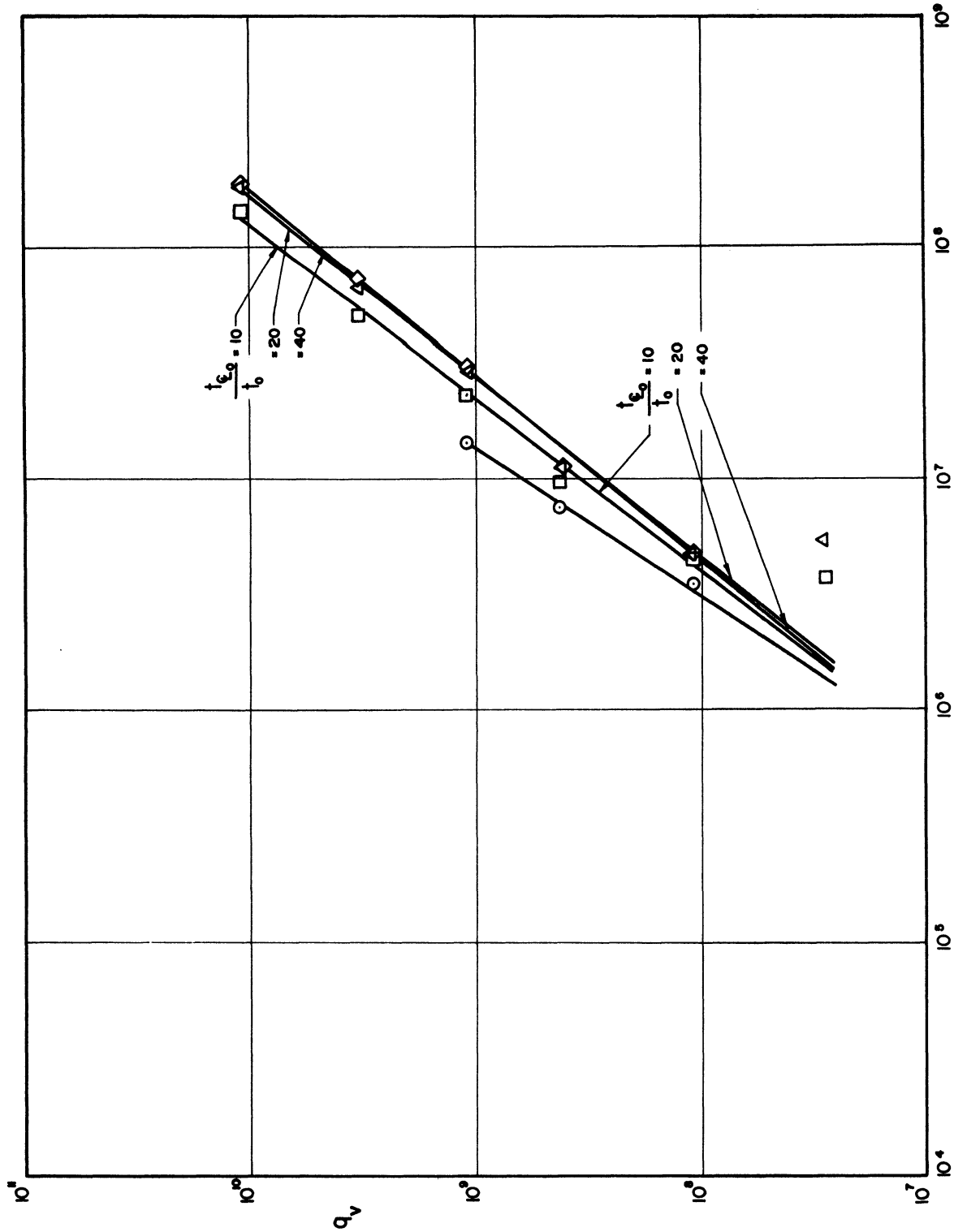

Figure 6. Non-Dimensional Heat Source vs. Overall Temperature Differential, Experimental Data.

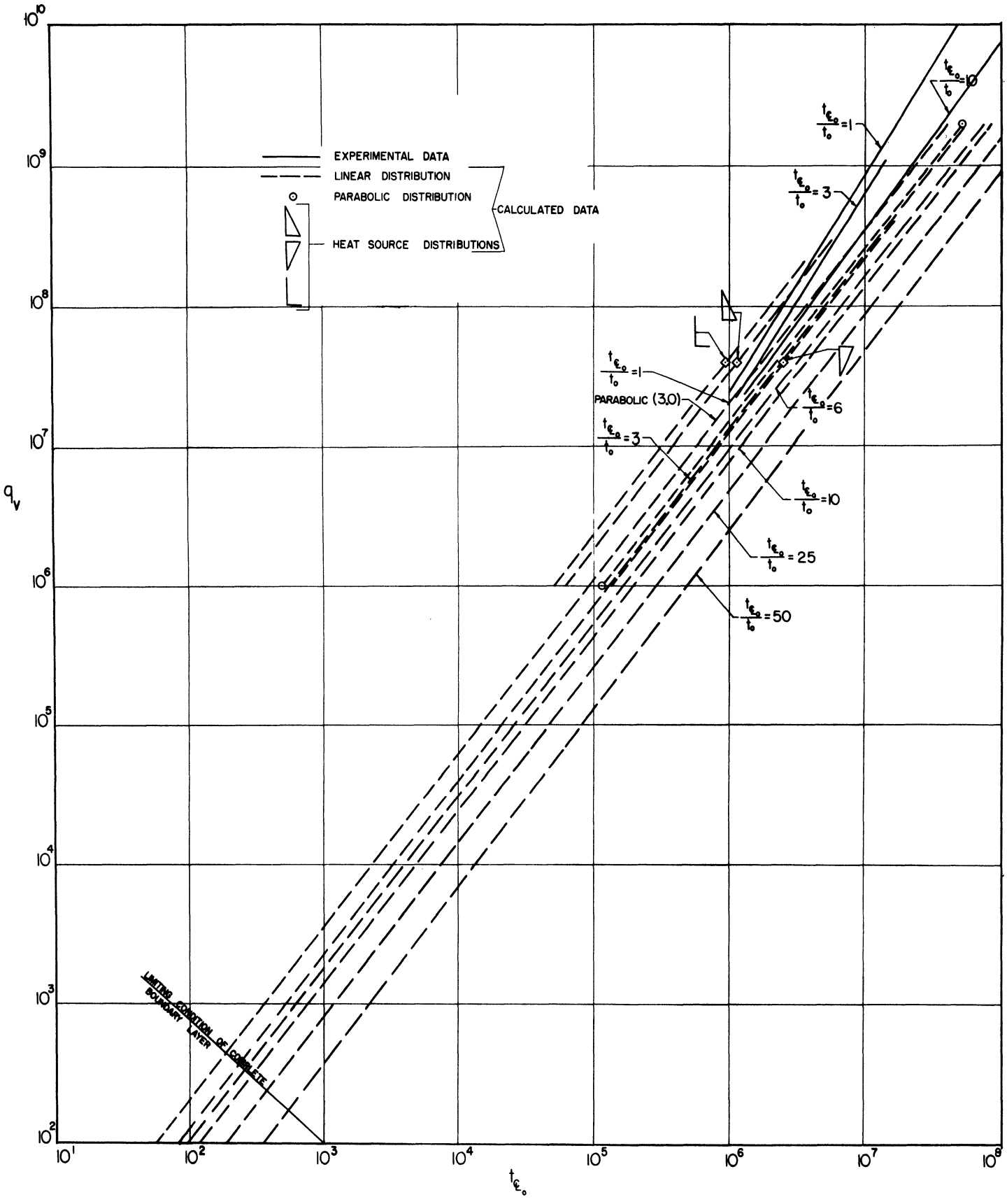

Figure 7. Non-Dimensional Heat Source vs. Overall Temperature Differential, Experimental and Calculated Data.

Detailed Comparisons

Axial and Radial Temperature Distributions

Figure 8 shows the comparison between the calculated axial temperature distribution in the fluid at the vessel centerline and the corresponding experimental data. The temperature differential between centerline and wall at a given axial position has been normalized by dividing by the overall temperature differential $t\not{\epsilon}_o$. A comparison is shown for constant wall temperature and also for $t\not{\epsilon}_o/t_o$ of 3.0. Since no experimental data was actually taken at constant wall temperature, this curve is an extrapolation from a cross-plot of t versus $t\not{\epsilon}_o/t_o$. The curve for $t\not{\epsilon}_o/t_o$ of 3.0 is also adjusted by cross-plot since the runs were made at fixed q_v rather than a fixed $t\not{\epsilon}_o/t_o$. The calculated centerline to wall temperature differential is less than that measured at most intermediate axial positions. It will be noted that in both cases, both experimental and analytical, the temperature differential between wall and centerline decreases rapidly in the lower portion of the vessel. This axial temperature gradient provides a basic difference between the vessel closed at both ends and that open to an infinite reservoir at one end.(1)

The computed curves of Figure 9 show the effect on the temperature of the various heat source distributions. Comparison is made with the uniform q_v curve. All curves are for constant wall temperature. As might be expected, a proportionate preponderance of heat source near the top results in a more gradual decrease of the centerline to wall differential. The curve marked $\llcorner$ applies to all heat added in a differentially

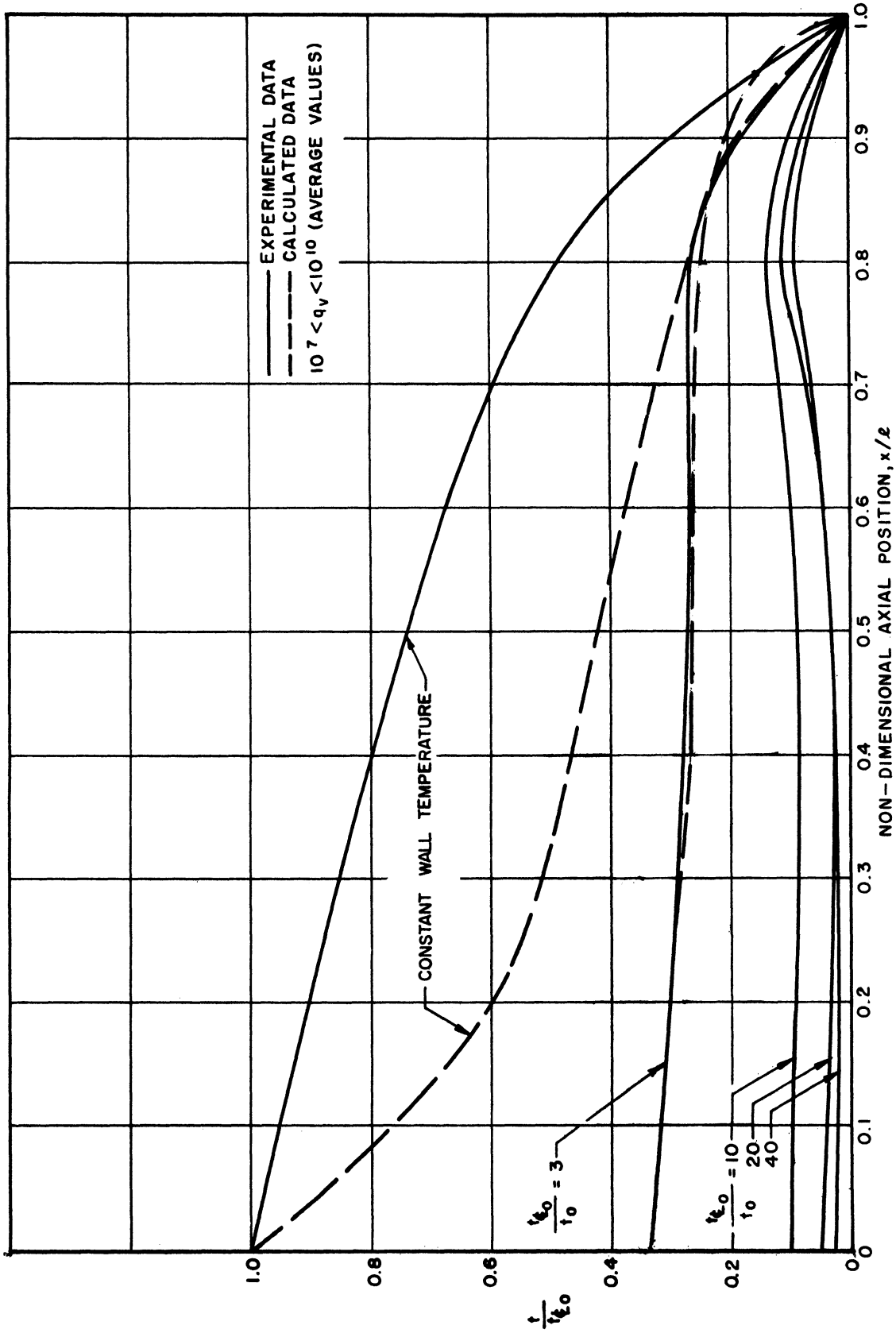

Figure 8 Non-Dimensional Temperature Differential Centerline to Wall vs. Non-Dimensional Axial Position.

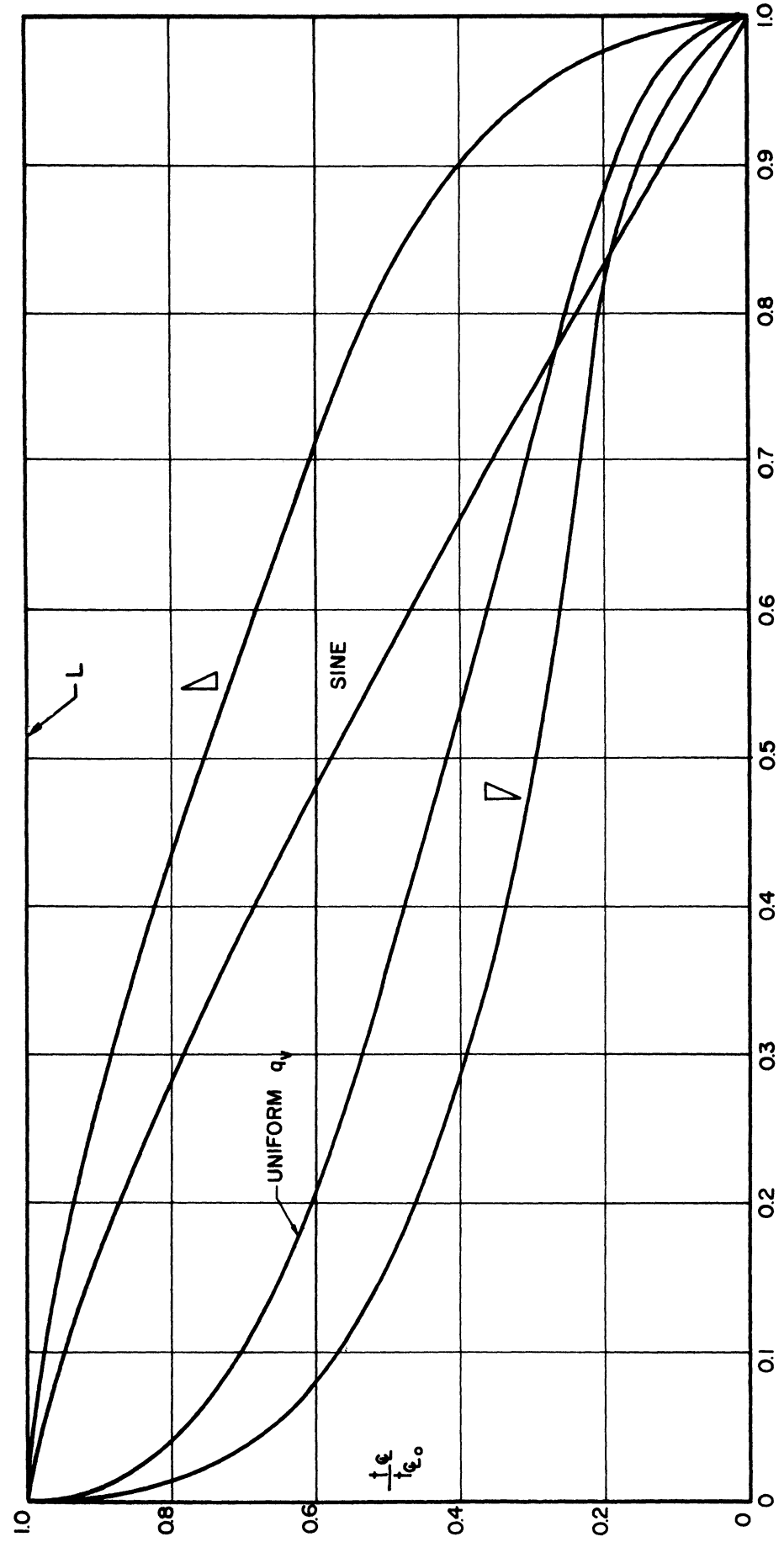

Figure 9. Non-Dimensional Centerline Temperature Distribution vs. Non-Dimensional Axial Position, Constant Wall Temperature, Various Axial Heat Source Distributions. $q_v = 4 \times 10^7$

thin disc at the bottom, and hence shows a constant (maximum) center-line temperature throughout the vessel length. This is equivalent to the infinite reservoir case of reference 1.

Boundary Layer Thickness

Figure 10 shows the variation of the boundary layer thickness as heat source strength and distribution are changed. With these latter as parameters the non-dimensional boundary layer thickness is plotted against axial position. It is noted that the boundary layer thickness is zero at the top ($x/l = 0$), increases to a maximum near the bottom of the tube, and very rapidly decreases again to zero at the bottom. Vanishing of the boundary layer at either end is a result of the flow model assumed. At the top it is consistent with the ordinary boundary layer concept, if it is assumed that the top of the wall is in effect a leading edge. However, the flow model is not sufficiently sophisticated to consider the detailed end effects realistically. Since the analysis shows the boundary layer to attain a significant thickness a very short distance from either end, its assumed disappearance at the mathematical end-points probably does not significantly affect the overall results.

Figure 10 shows that the maximum boundary layer thickness attained is inversely related to q_V. It fills the entire tube for q_V of the order of 10^2 to 10^3 .[5] The boundary layer limit, Figure 1, is defined as that point where the velocity profile attains zero slope and an upward velocity equal to the core velocity. Thus the

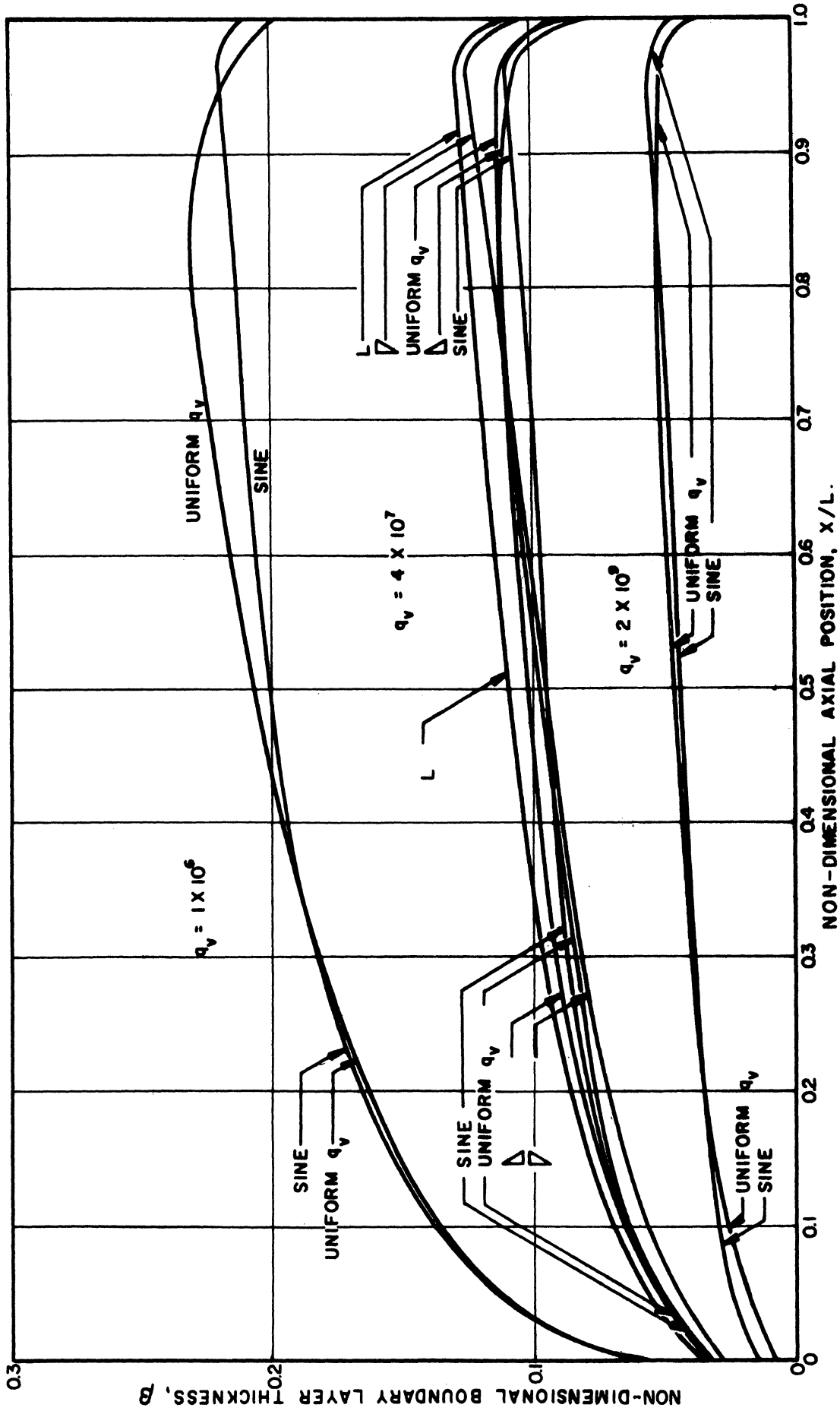

Figure 10. Non-Dimensional Boundary Layer Thickness vs. Non-Dimensional Axial Position, Constant Wall Temperature, Uniform Heat Source, Calculated Data.

boundary layer as here used includes upward flow. When the boundary layer fills the entire cross-section, the flat portion of the velocity profile is eliminated and the profile is continuous across the tube attaining zero slope only at the centerline.

No accurate experimental measurements of boundary layer thickness have been possible. However, by the injection of dye at a known location, the approximate location of the interface between upward and downward velocity components has been estimated.

Also the extent of the temperature boundary layer (where the temperature profile attains zero slope and a value equal to the core temperature - see Figure 1) can be estimated from the experimental data, as Figure 4. It was assumed in the analysis that the temperature and velocity boundary layers are of equal extent. The present data show that this assumption is at least approximately correct for water.

Figure 11 shows a comparison of the temperature boundary layer estimates with the computed data. The order of magnitudes compare within reason, but due to the insufficient number of observations and inherent lack of precision in the method, no definitive statements can be made. No observations of boundary layer thickness very near the ends of the vessel are available.

Fluid Velocity

The computed non-dimensional fluid velocities for constant wall temperature are shown in Figure 12 for both the boundary layer (maximum velocity is shown) and the core. As expected the velocities increase with

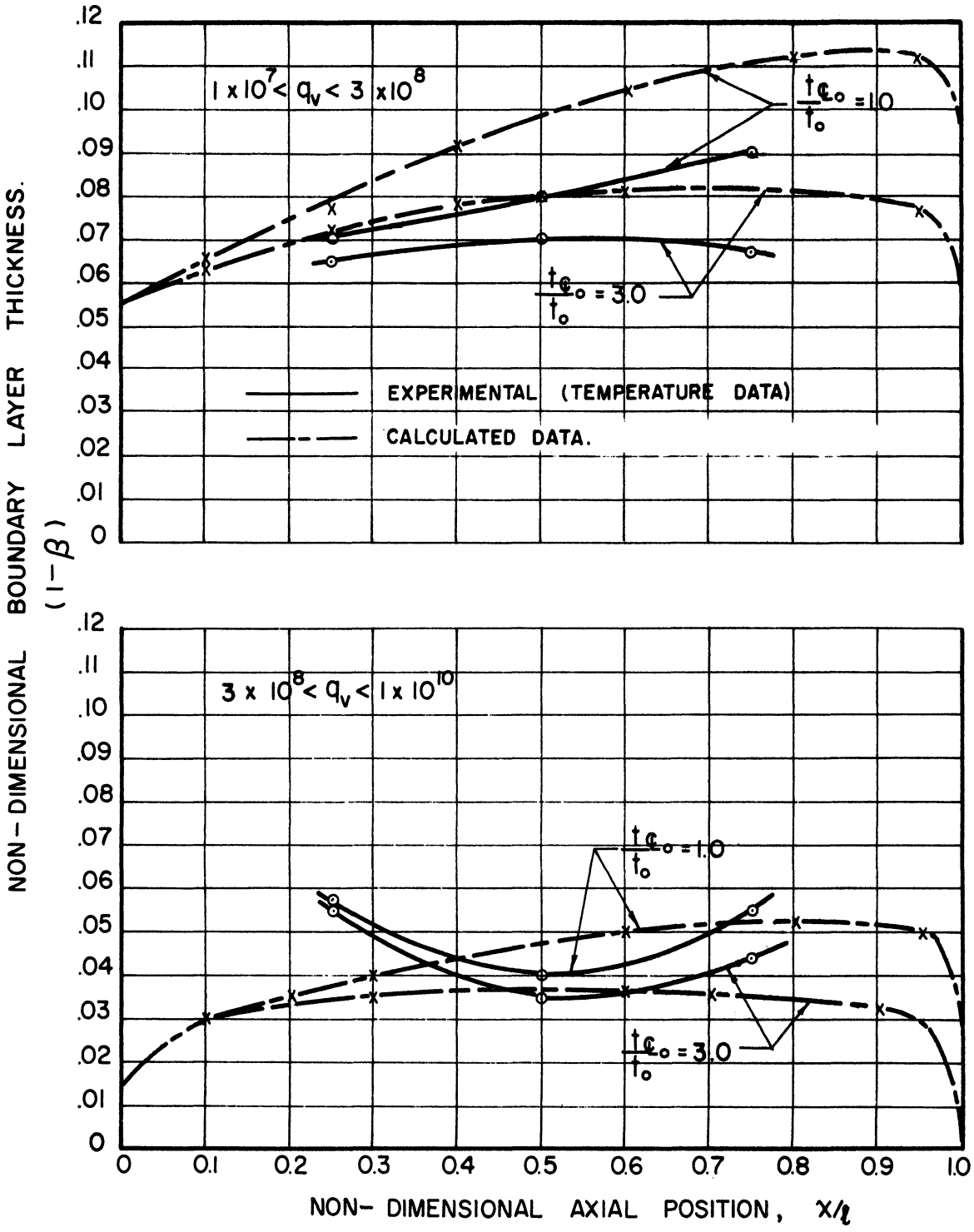

Figure 11. Non-Dimensional Boundary Layer Thickness vs. Non-Dimensional Axial Position.

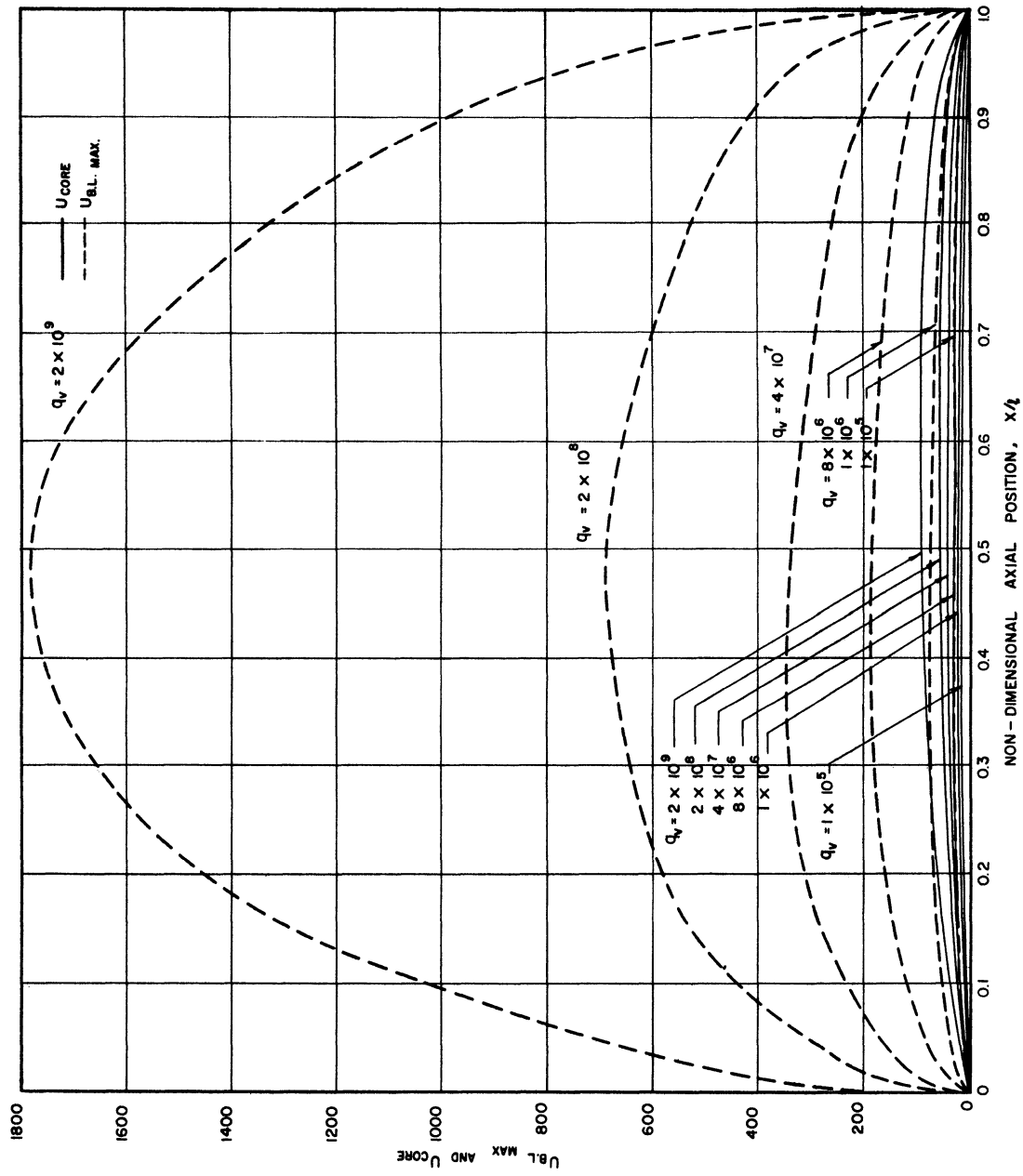

Figure 12. Non-Dimensional Core and Boundary Layer Velocity vs. Non-Dimensional Axial Position, Uniform q_v, Constant Wall Temperature, Calculated Data.

increased q_v. For high q_v the boundary layer velocity is much greater than the core velocity whereas at low q_v[5] the situation is reversed. This is inherent in the assumed type of profile and may not be physically meaningful for low q_v. The curves for variable wall temperature (not shown) are similar. The effect of a wall temperature gradient is to reduce the velocities at a given heat source value.

Velocity observations were made by injecting dye at a known location and timing its motion. Such observations are at best semi-quantitative. As a matter of interest, velocities of the order of 1 inch per second were observed in the water-cooled facility at maximum heat input.

A comparison between the observations averaged at several q_v and so plotted, and the calculated data is shown in Figure 13. It is noted that the observed boundary layer velocity is less than that computed, and the observed core velocity greater. The fact that the observed boundary layer velocities were less than the calculated may be explained by turbulent mixing with the upward moving core, and also by the fact that the observation necessarily involves a mean downward velocity while the calculation is based on the maximum of the assumed parabolic profile. The fact that the observed core velocities were higher than calculated may perhaps be explained on the basis that the assumed flat core velocity profile is not realized and velocities significantly larger than such a "mean" value must exist if continuity is to be observed.

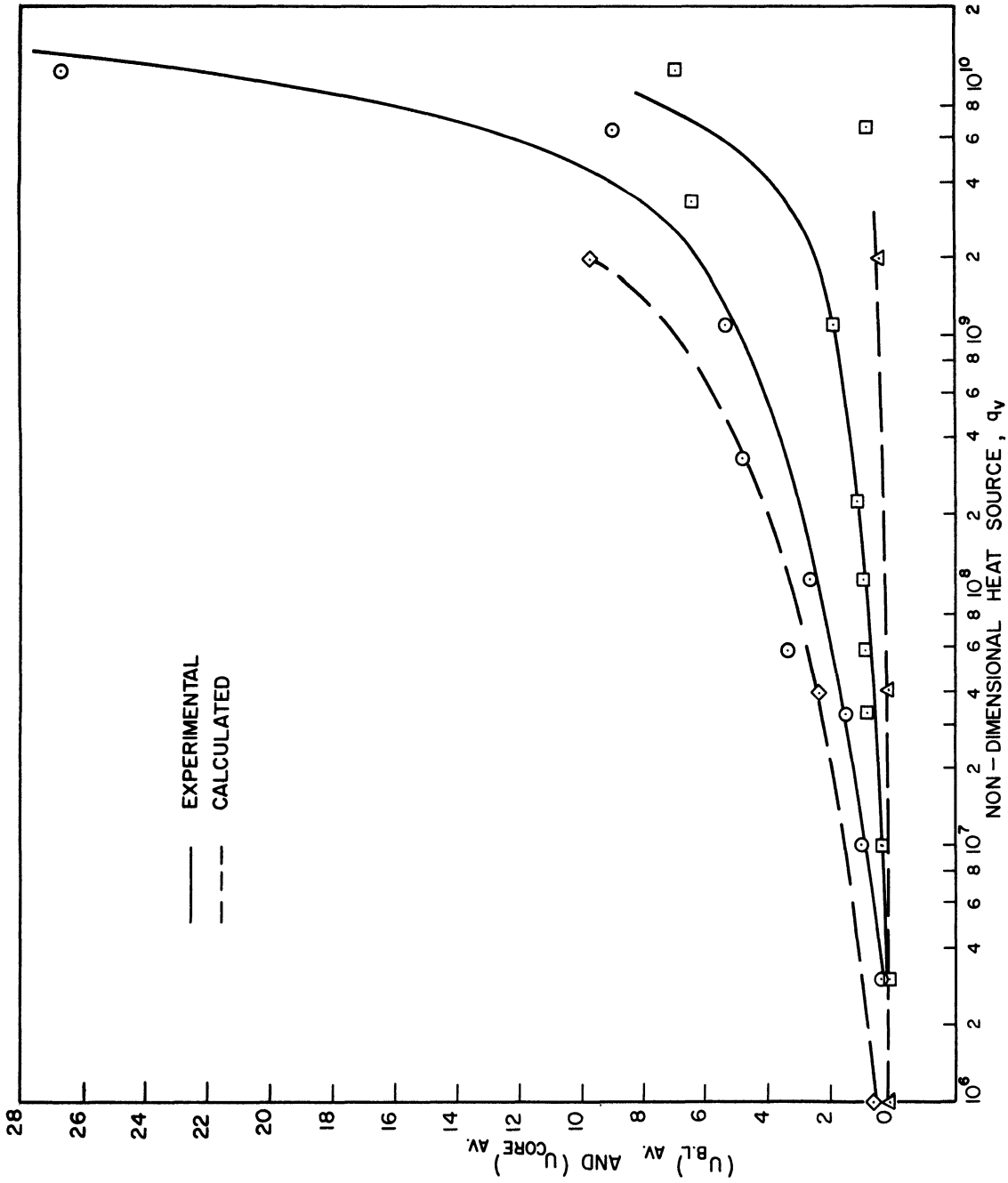

Figure 13. Non-Dimensional Boundary Layer and Core Velocity vs. Non-Dimensional Heat Source, Comparison of Experimental and Calculated Data.

Wall Heat Flux Distribution

The heat conduction through the wall, integrated over the vessel, is of course equal to the total heat source. If an infinitely long vessel were assumed, so that end effects were negligible, a local equality between wall heat flux and heat source would prevail. However, this is not the case for vessels short enough so that end effects are important.

The wall heat flux is influenced by the temperature differential between centerline and wall at a given axial position and also by the boundary layer thickness at that position. On both accounts a peak value would be expected near the top and a corresponding decrease in the lower portion.

The computed wall heat flux distribution for uniform heat source and constant wall temperature is shown in Figure 14. The heat flux values are normalized to the value at the $x/\ell = 0.5$ position. Under these conditions the average value attained in the uppermost 10% of the vessel is approximately 6 times the value at the midpoint and the value in the lower 10% about 0.4 times the midpoint value. Reducing q_v does not affect the extremes but rather tends to level out the central portion. In any case the distribution is quite insensitive to q_v.

The effect of wall temperature gradient is shown in Figure 15. At a given q_v a more severe wall temperature gradient results in a reduction of the extremes and a much more severe leveling of the central portion.

Wall heat fluxes were observed at x/ℓ positions of 0.25, 0.5, and 0.75 by measuring the temperature drop across the wall. The comparison

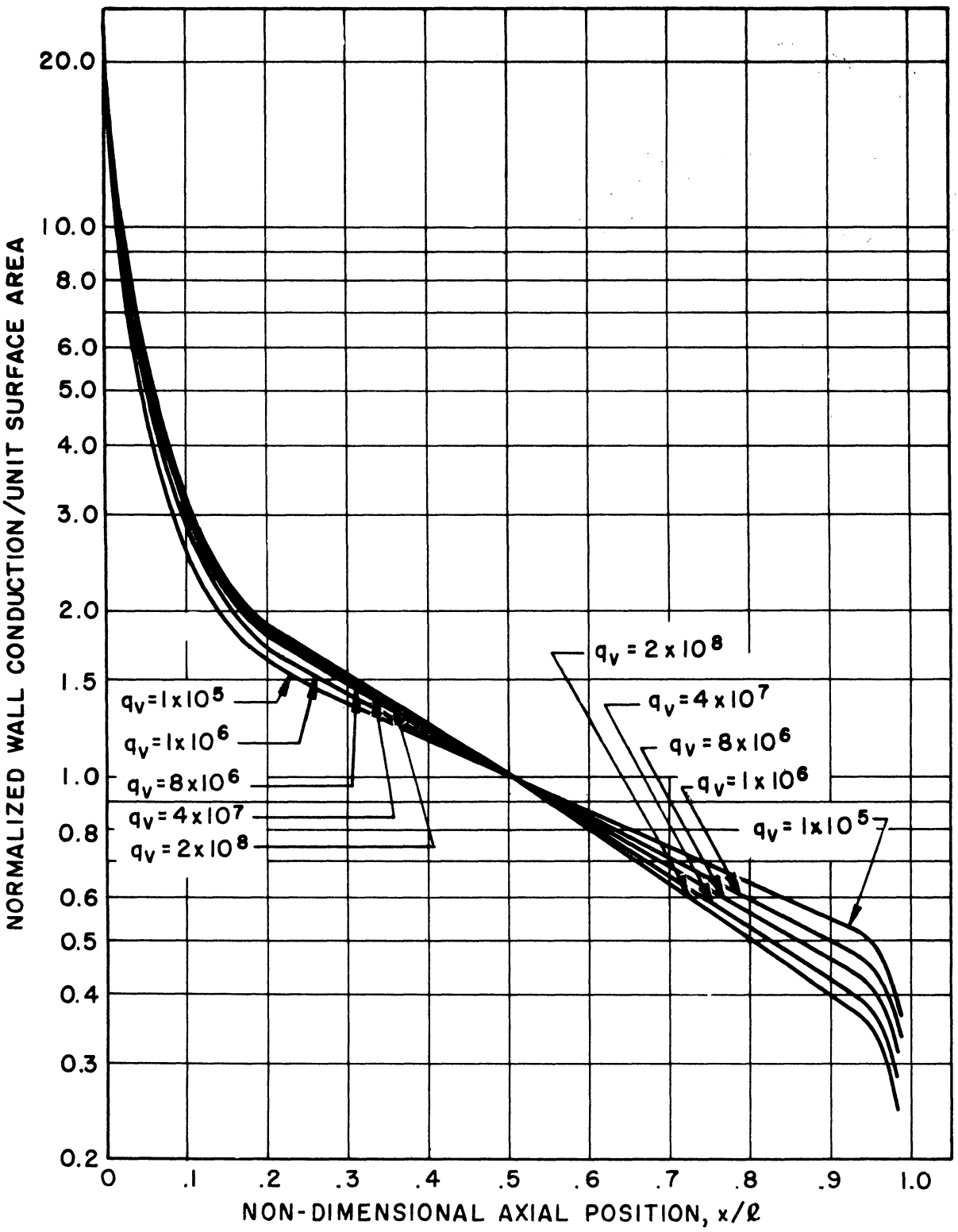

Figure 14. Normalized Wall Conduction vs. Non-Dimensional Axial Position, Constant Wall Temperature, Uniform Heat Source Distribution.

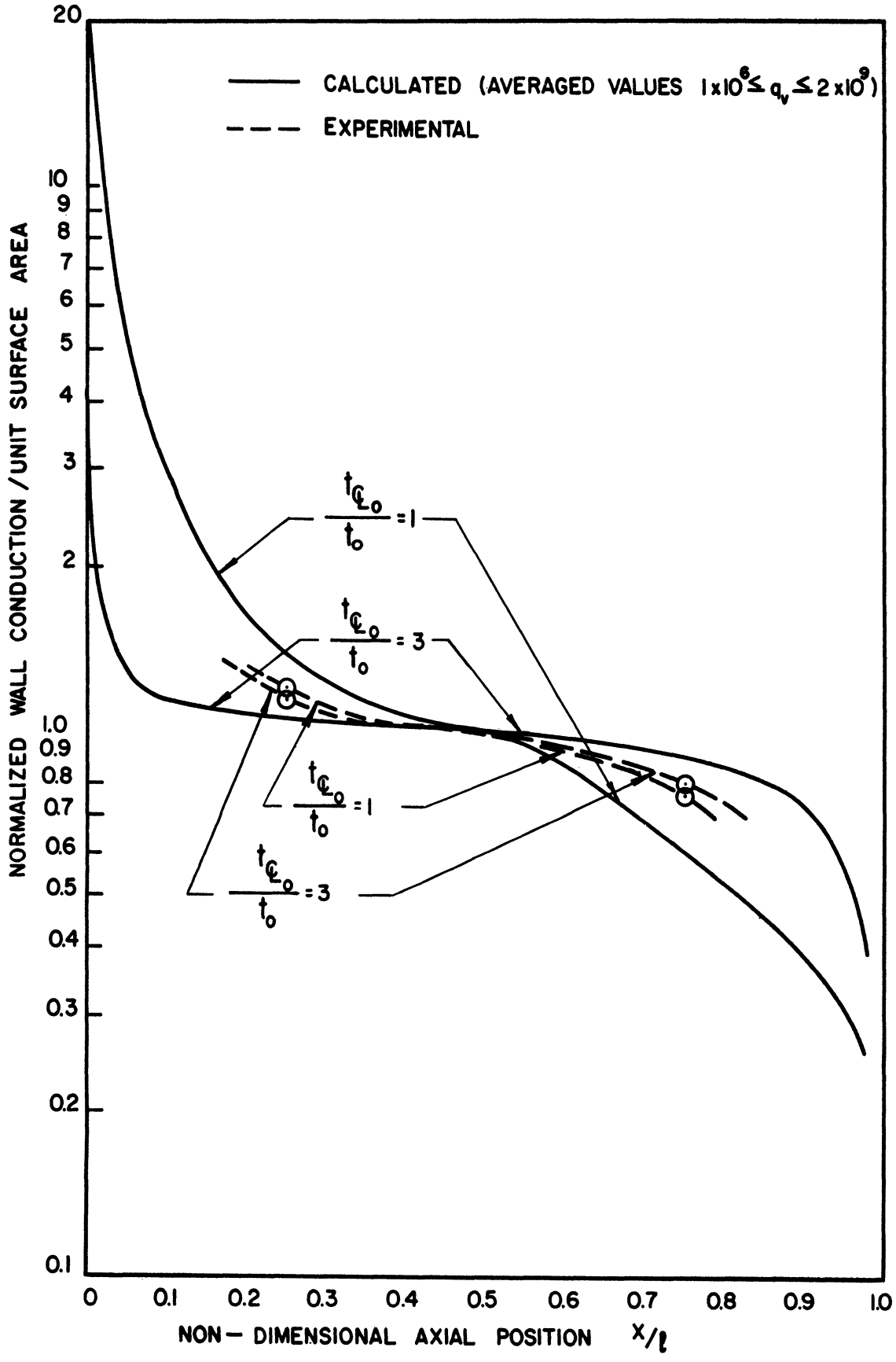

Figure 15. Normalized Wall Conduction vs. Non-Dimensional Axial Position, Linear Wall Temperature Distribution, Calculated and Experimental Comparison, Uniform Heat Source.

between the observed and calculated values are included on Figure 15. The observed non-uniformity of wall heat flux, like the calculated, decreases with increasing wall temperature gradient, although slightly more than the calculated value. No observations near the ends, where the more gross effects are predicted, were possible since the test section wall thickness was such that axial conduction in the glass would have obscured the effect had it existed.

CONCLUSIONS

An analysis of laminar flow under the influence of natural convective forces in a closed-end vertical cylindrical vessel wherein heat is generated internal to the fluid and removed through the container walls is presented. The solution includes arbitrary axial distribution of wall temperature and heat source. Calculated data derived from a numerical procedure programmed into a high-speed digital computer are shown for a variety of cases.

In addition, experimental data covering a wide range of vessel size, length to diameter ratio, heat source strength, and wall temperature distribution is presented. It is concluded that there is good agreement between the analysis and observations so far as the magnitude and direction of changes in dependent variables caused by changes in the independent variables is concerned. This agreement includes the local temperatures and velocities to be found within the fluid. However, the observed overall temperature differentials to remove a given quantity of heat are less than those predicted by a factor of about 2.5 for the higher heat source strengths and 1.5 for the lower. The discrepancy is believed to be the result of turbulence which was present in the experiments but not considered in the analysis. The observations covered a range of approximately 10^3 in the non-dimensional heat source parameter while the calculations cover a range of 10^7.

It is felt that a realistic basis has been provided for the estimation of overall heat transfer, local velocities, and local temperatures over a very wide range of conditions for the application investigated.

The approximate application of the analytical results over a wide range is justified by the demonstrated relation between experiment and analysis over a smaller range.

Observations disclosed the appearance of substantial degrees of turbulence for Ra_a greater than about 4.0×10^7.

NOMENCLATURE

a Radius of test section

c_v Specific heat

g Acceleration of gravity

h Film coefficient for heat transfer

k Thermal conductivity

ℓ Length of test section

Nu_a Nusselt's Number based on radius; $\frac{ha}{k}$

Pr Prandtl Number; $\frac{\nu}{\kappa}$

q_v Non-dimensional volumetric heat source $\frac{Q_v a^6 \alpha g}{\rho^2 \kappa^2 \ell c_v}$

Q_v Volumetric heat source -- energy per unit volume

Ra_a Rayleigh Number based on radius and maximum temperature differential;

$$\frac{\alpha g a^3 (\Delta T_{Max \, ℄ \text{ to Wall}})}{\nu \kappa}$$

Ra_ℓ Rayleigh Number based on length and maximum temperature differential;

$$\frac{\alpha g \ell^3 (T_{Max \, ℄ \text{ to Wall}})}{\nu \kappa}$$

R, r Dimensional and non-dimensional coordinates in radial direction

T Temperature

t Non-dimensional temperature differential = $\frac{\alpha g a^4 \Delta T}{\nu \kappa \ell}$; without subscript non-dimensional temperature differential between wall and fluid at any given axial position. Subscript o applies to top of tube centerline. Subscript ℄ applies to centerline. $Nu_a = q_v/2t_{℄_o}$.

U Velocity in axial direction

NOMENCLATURE (CONT'D)

u	Non-dimensional velocity in axial direction = $a^2U/\kappa\ell$
X,x	Dimensional and non-dimensional coordinates in axial direction
α	Coefficient of volumetric expansion
β	Non-dimensional core thickness. $1 - \beta$ is non-dimensional boundary layer thickness.
κ	Thermal diffusivity = $k/\rho c_v$
ν	Kinematic viscosity
ρ	Density

BIBLIOGRAPHY

1. Lighthill, M. J., "Theoretical Considerations on Free Convection in Tubes," Quarterly Journal of Mechanics and Applied Mathematics, Vol. 6, 1953, pp. 398-439.

2. Hammitt, F. G., "Modified Boundary Layer Type Solution for Free Convection Flow in Vertical Closed Tube with Arbitrary Distributed Internal Heat Source and Wall Temperature," ASME paper number 58-SA-30, Semi-Annual Meeting, Detroit, Michigan, June 15-19, 1958.

3. Hammitt, F. G., "Heat and Mass Transfer in Closed, Vertical, Cylindrical Vessels with Internal Heat Sources for Homogeneous Nuclear Reactors," Ph.D. Thesis, University of Michigan, Ann Arbor, Michigan, December 1957.

4. Haas, P. A., and Langsdon, J. K., "HRP-CP Heat Removal from a Proposed Hydroclone Underflow Pot Geometry for a Volume Heat Source," CF-55-10-7, Oak Ridge National Laboratory, December 3, 1954.

5. Brower, E. M., "Heat and Mass Transfer in Closed Cylindrical Passage of Homogeneous Nuclear Reactors with Internal Heat Generation," Master's Thesis in Nuclear Engineering, University of Michigan, Ann Arbor, Michigan, April 1958.

6. Mohr, Dale, "Evaluation of the Prandtl Number Error in the Modified Boundary Layer Type Solution for Free Convection Flow in Vertical Closed Tube with Arbitrarily Distributed Internal Heat Source and Wall Temperature," Master's Thesis in Nuclear Engineering, University of Michigan, Ann Arbor, Michigan, June, 1958.